Spatial Structures and Giant Number Fluctuations in Models of Active Matter

Supravat Dey,[1] Dibyendu Das,[1] and R. Rajesh[2]
[1]Department of Physics, Indian Institute of Technology, Bombay, Powai, Mumbai-400 076, India*
[2]Institute of Mathematical Sciences, CIT Campus, Taramani, Chennai-600113, India
(Received 21 February 2012; published 4 June 2012)

The large scale fluctuations of the ordered state in active matter systems are usually characterized by studying the ''giant number fluctuations'' of particles in any finite volume, as compared to the expectations from the central limit theorem. However, in ordering systems, the fluctuations in density ordering are often captured through their structure functions deviating from Porod's law. In this Letter we study the relationship between giant number fluctuations and structure functions for different models of active matter as well as other nonequilibrium systems. A unified picture emerges, with different models falling in four distinct classes depending on the nature of their structure functions. For one class, we show that experimentalists may find Porod's law violation, by measuring subleading corrections to the number fluctuations.

DOI: 10.1103/PhysRevLett.108.238001 PACS numbers: 45.70.Qj, 74.40.Gh

Active matter, collections of interacting self-propelled particles, are found in many different contexts. Examples include bird flocks [1], bacterial colonies [2], actin filaments propelled by molecular motors [3], and vibrated granular rods and disks [4–6]. In these, the ''activity'' refers to conscious decision making or internally generated cellular thrusts in the biological systems and impulses from a vibrating plate for the granular systems. The combination of activity and interaction can lead to macroscopic order [7–12]. However, these systems are far from equilibrium and the usual notions of equilibrium phase transitions come under unexpected challenges [13,14]. In particular, macroscopic order and large scale fluctuations reminiscent of critical equilibrium systems coexist.

Depending on their dynamics and symmetries, different active matter systems exhibit macroscopic polar, nematic, and/or density order. Polar ordering has been demonstrated in point polar particle (PP) models [7,9], experiments with granular disks [6], and continuum theories [13,14]. For polar rods (PR), continuum theories rule out macroscopic polar ordering [15], and experiments on mobile bacteria [2] and simulations of models of polar rods are in agreement [11,16]. Apolar rods (AR), or active nematics, have been studied experimentally [4], in hydrodynamic theories [14,17], and in simulation [10] and exhibit nematic and density ordering.

The density fluctuations in the ordered state have been characterized by the number fluctuations $\sigma_l^2 = \langle N^2\rangle - \langle N\rangle^2$ of particles in a finite box of linear size l, where N is the particle number. In active matter systems, $\sigma_l^2 \sim \langle N\rangle^\alpha$ with $\alpha > 1$, indicating ''giant'' number fluctuations (GNF) in comparison to what is expected from the central limit theorem. The exponent α has been used to infer the long-range correlations in the system. In two dimensions, for the PP [6,9,14] and PR [2,11] systems, it is now known that $\alpha = 1.6$, and for the AR systems [4,14,17] $\alpha = 2.0$.

Consider now an active matter system relaxing to its ordered state from an initial disordered state. As the density order grows with time t, there is an increasing macroscopic length scale $\mathcal{L}(t)$ over which there is enhanced clustering. Information about the spatial structures in such a coarsening system can be obtained by studying the spatial density-density correlation function $C(\mathbf{r}, t) = \langle\rho(\mathbf{0}, t)\rho(\mathbf{r}, t)\rangle$, where $\rho(\mathbf{r}, t)$ is the local density at point $\mathbf{r}$. Systems relaxing to an equilibrium state typically exhibit clean domain formation [18], resulting in a linear form of $C(\mathbf{r}, t) = a - b|\mathbf{r}|/\mathcal{L}(t)$ for $|\mathbf{r}|/\mathcal{L}(t) \ll 1$, known as Porod's law [19]. On the other hand, many systems relaxing to a nonequilibrium steady state violate Porod's law due to a hierarchy of cluster sizes. Examples include sliding particles on fluctuating interfaces [20] and freely cooling granular gases [21].

In this Letter, we ask the following. First, we ask whether coarsening active matter systems obey Porod's law. A few studies have addressed this question—discrete models of active nematics [22] and a recent numerical implementation of a hydrodynamic polar model [23] have shown non-Porod behavior. A further systematic study is necessary, and in this Letter we show that Porod's law is indeed violated by all the models that we study.

Second, we ask whether the fluctuations that contribute to GNF are the same as those that cause Porod's law to be violated. In particular, we ask whether the large distance behavior of $C(\mathbf{r}, t)$ can be deduced by knowing α. In general, $C(\mathbf{r}, t)$ contains more information than σ_l^2, as the latter is derived from the former:

$$\sigma_l^2(t) = l^d \int_0^l d^d\mathbf{r}[C(\mathbf{r}, t) - \langle\rho\rangle^2], \tag{1}$$

where $\langle\rho\rangle$ is the mean density. If the integrand decays to zero over a length scale $\xi \ll l$, then $\sigma_l^2(t) \sim l^d \sim \langle N\rangle$ for large l, or $\alpha = 1$. Since $\alpha > 1$ for active matter, the upper limit of Eq. (1) should contribute to the integral, implying that nontrivial correlations extend beyond the scale $\mathcal{L}(t) \geq l$. Hence, one would expect the behavior of $C(\mathbf{r}, t)$ near $|\mathbf{r}|/\mathcal{L}(t) \approx 1$ to contribute to $\sigma_l^2(t)$ in Eq. (1), but we will see below many interesting exceptions to this. In this Letter, we show that different active matter systems as well as other nonequilibrium systems studied in other contexts, fall into four distinct classes based on the relation between their $\sigma_l^2(t)$ and $C(\mathbf{r}, t)$. In the case of the first type, the small $|\mathbf{r}|/\mathcal{L}(t) \ll 1$ behavior of $C(\mathbf{r}, t)$ has no bearing on the exponent α. For the other three types, it does, albeit in three distinct ways.

Type 1.—We start with PP systems. We first study numerically the Vicsek model [7], which we denote as PP(1), in two dimensions. All particles move with constant speed v_0. The positions $\mathbf{r}_i$ and velocity orientations θ_i of particle i at time $t + \Delta t$ are given by $\mathbf{r}_i(t + \Delta t) = \mathbf{r}_i(t) + \mathbf{v}_i(t)\Delta t$, and $\theta_i(t + \Delta t) = \arg[\sum_k \exp(i\theta_k(t))] + \Lambda\xi(i, t)$, where the summation over k is restricted to those satisfying $|\mathbf{r}_k - \mathbf{r}_i| < R$, and ξ is white noise over the range $(-\pi, \pi]$. It is known that the system undergoes a transition from an ordered state to a disordered state as the noise strength Λ is increased [7].

We choose parameter values for which the steady state is polar ordered with no density bands and study numerically the density structures in the coarsening regime—a typical snapshot of the density clusters in shown in Fig. 1(a). In the time regime studied, $C(\mathbf{r}, t)$ has no directional anisotropy. Hydrodynamic theory predicts a length scale $\mathcal{L}(t) \sim t^{5/6}$ [8,14]. Interestingly, we find that $C(\mathbf{r}, t)$ and the corresponding scaled structure function $S(k, t)/\mathcal{L}^2$ [see Fig. 1(b)] show a data collapse for a completely different coarsening length $\mathcal{L}(t) \sim t^{\gamma}$ with $\gamma = 0.25 \pm 0.05$. To understand the physical origin of this length scale, we studied the two eigenvalues λ_1 and λ_2 of the inertia tensor of the largest cluster. Both of these grow as $\sim t^{0.5}$ [see Fig. 1(c)], implying that the radius of the largest cluster grows as $t^{0.25}$, determining the length scale $\mathcal{L}(t)$. The $S(k, t)$ [Fig. 1(b)] consists of two distinct power laws with exponents -1.2 for small $k\mathcal{L}(t)$ and -2.6 ± 0.1 for large $k\mathcal{L}(t)$; the former has been known in hydrodynamic theory [8], but we highlight the latter, signifying violation of Porod's law. In real space, the latter implies that $C(\mathbf{r}, t)$ has a cusp of the form $a - b|\mathbf{r}/\mathcal{L}(t)|^{\beta_1}$ with $\beta_1 = 0.6 \pm 0.1$ for $|\mathbf{r}|/\mathcal{L}(t) \ll 1$, and a second power law $|\mathbf{r}|^{-\eta}$ with $\eta = 0.8 \pm 0.1$ for $|\mathbf{r}|/\mathcal{L}(t) \geq 1$. Due to this crossover, the GNF exponent α, determined from Eq. (1), depends only on the exponent η:

$$\alpha = 2 - \eta/d. \tag{2}$$

In the coarsening regime, from a direct measurement of σ_l^2, we find $\alpha = 1.6$ [see Fig. 1(d)], consistent with Eq. (2), and measurements in the steady state [6].

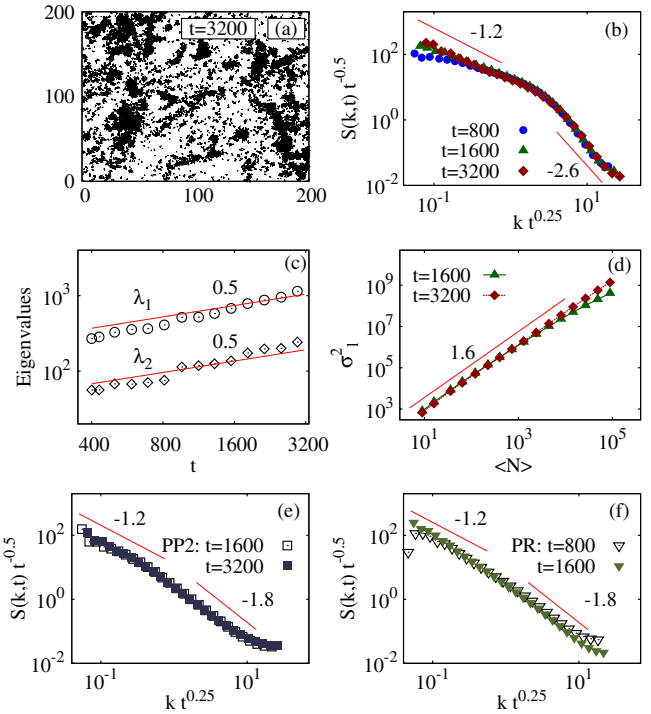

FIG. 1 (color online). (a)–(d): Simulation results for the PP(1) model (system size 1024×1024, $\rho = 1.0$, $v_0 = 0.5$, and $\Lambda = 0.3$). (a) Snapshot of a part of the system at $t = 3200$ showing the domain structure. (b) Plot of scaled structure function decays as a power law with exponents -2.6 [large $k\mathcal{L}(t)$] and -1.2 [small $k\mathcal{L}(t)$]. (c) The eigenvalues of the inertia tensor for the largest cluster grow as $\sim t^{0.5}$. (d) Variance of number $\sigma_l^2 \sim \langle N\rangle^{1.6}$. (e) PP(2) model [parameters same as PP (1)]: scaled structure function decays as a power law with exponents -1.8 [large $k\mathcal{L}(t)$] and -1.2 [small $k\mathcal{L}(t)$]. (f) PR model (system size 1024×1024, $\rho = 1.0$, $v_0 = 0.5$, and $\Lambda = 0.2$): scaled structure function decays as a power law with exponents -1.8 [large $k\mathcal{L}(t)$] and -1.2 [small $k\mathcal{L}(t)$].

Interestingly, the structure functions in two other polar models have the same qualitative behavior. A modified version of the PP(1) model was studied in Ref. [9], which we refer to as PP(2) model. The rules of the PP(2) model are the same as those of the PP(1) model except that the new positions depend on the new velocities: $\mathbf{r}_i(t + \Delta t) = \mathbf{r}_i(t) + \mathbf{v}_i(t + \Delta t)\Delta t$. Most macroscopic features remain the same as PP(1), except that the steady state configurations have density bands [9]. In the time regime that we study, $C(\mathbf{r}, t)$ is isotropic and bands do not form. The structure function is shown in Fig. 1(e)—we find, as in PP(1), $\mathcal{L}(t) \sim t^{0.25}$ and the small $|\mathbf{k}|\mathcal{L}(t)$ behavior implies $\eta = 0.8$. However, for large $|\mathbf{k}|\mathcal{L}(t)$, $S(\mathbf{k}, t)$ is a distinct power law with exponent -1.8, implying a "divergence" (as opposed to a cusp) of $C(\mathbf{r}, t)$ for small $|\mathbf{r}|/\mathcal{L}(t)$ as $|\mathbf{r}/\mathcal{L}(t)|^{-\beta_2}$, with $\beta_2 = 0.2 \pm 0.1$—again showing non-Porod behavior.

Next, we studied a PR model defined in Ref. [11]. The time evolution of the θ_i's in the PR model differs from that

in the PP(2) model: $\theta_i(t+\Delta t) = \arg[\sum_k \mathrm{sign}[\cos(\theta_k(t) - \theta_i(t))]\exp(i\theta_k(t))] + \Lambda\xi(i,t)$ and $\Lambda \in (-\pi/2, \pi/2]$. We find that the scaling of $\mathcal{L}(t)$, as well as the shape of $S(\mathbf{k}, t)$ of the PR model, is similar to the PP(2) model [see Fig. 1(f)].

In summary, the models PP(1), PP(2), and PR share the following common features. They have a coarsening length scale $\mathcal{L}(t) \sim t^{0.25}$. At small $|\mathbf{r}|/\mathcal{L}(t)$, the correlation functions violate Porod's law either as a cusp or as a power law divergence. For large $|\mathbf{r}|/\mathcal{L}(t)$, they exhibit a generic second power law decay with exponent $\eta = 0.8$, which determines the GNF exponent $\alpha = 1.6$. Thus, for polar models (type 1), the non-Porod behavior and the GNF characterize distinct sources of fluctuation.

Type 2.—We study the discrete AR model introduced in Ref. [10]. The θ_i's now evolve as follows. The traceless two dimensional matrix $Q_{jk} = \langle v_j v_k\rangle - \frac{1}{2}\delta_{jk}$ (with v_j denoting the components of the unit velocity vectors) is calculated, where the average is done over the particles that are in the disk of radius R, centered about particle i. If $\bar{\Theta}$ denotes the direction of the largest eigenvector of Q, then $\theta_i(t+\Delta t) = \bar{\Theta} + \Lambda\xi(i,t)$, with $\Lambda \in (-\pi/2, \pi/2]$. The positions $\mathbf{r}_i(t+\Delta t) = \mathbf{r}_i(t) \pm \mathbf{v}_i(t+\Delta t)\Delta t$, with the signs being chosen randomly with equal probability. The steady state of the AR model is characterized by nematically ordered bands; however, in the coarsening regime that we study, they do not arise. Instead, very interesting cell-like structures—low density zones with high density contours—form [see Fig. 2(a)], whose radii increase with time. The data for $C(\mathbf{r}, t)$ and $S(\mathbf{k}, t)/\mathcal{L}^2$ for different times collapse when plotted against $|\mathbf{r}|/\mathcal{L}(t)$ or $|\mathbf{k}|\mathcal{L}(t)$, with $\mathcal{L}(t) \sim t^{0.5}$ [see Figs. 2(b) and 2(c)]. We make an independent estimate of $\mathcal{L}(t)$ by counting the number of cell-like zones, thus measuring the mean cell radius $R_c(t)$. We obtain $\mathcal{L}(t) \sim R_c \sim t^{0.5}$ [see Fig. 2(d)]. For $|\mathbf{r}|/\mathcal{L}(t) \ll 1$, $C(\mathbf{r}, t) \sim a - b|\mathbf{r}/\mathcal{L}(t)|^{\beta_1}$ shows Porod's law violation with a cusp singularity $\beta_1 = 0.45 \pm 0.05$ determined from $S \sim k\mathcal{L}^{-2.45}$ [see Fig. 2(c)]. Unlike the PP models, there is no second power law regime in $C(\mathbf{r}, t)$ for $|\mathbf{r}|/\mathcal{L}(t) \gg 1$. The above cusp singularity of $C(\mathbf{r}, t)$ is similar to another discrete model of active nematics in two dimensions (see Fig. 5 of Ref. [22]) and a completely different model of particles sliding under gravity on a fluctuating interface in one dimension (see Fig. 2 of Ref. [20]). Due to the similar functional form of $C(\mathbf{r}, t)$, the number fluctuation from Eq. (1) is

$$\sigma_l^2 \sim a\langle N\rangle^2 - \frac{b}{\mathcal{L}^{\beta_1}}\langle N\rangle^{\beta_1/d+2} + \cdots \qquad (3)$$

The leading order behavior $\sigma_l^2 \approx \langle N\rangle^2$ is seen in our data for the AR model [see Fig. 2(e)], as well as for the sliding particle system [see Fig. 2(f)]. Thus, the scaling $\sigma_l^2 \sim \langle N\rangle^2$ may arise in systems other than active nematics. Even in an ordinary density phase segregating system with density 1/2 consisting of domains of equal length $\mathcal{L}(t)$, the correlation function is $1 - |r|/\mathcal{L}(t)$ (satisfying Porod's law) for $|r| < 2\mathcal{L}(t)$, and the number fluctuation is exactly $\sigma_l^2 = \langle N\rangle^2 - 4\langle N\rangle^3/\mathcal{L}(t) \approx \langle N\rangle^2$ for large $\mathcal{L}(t)$.

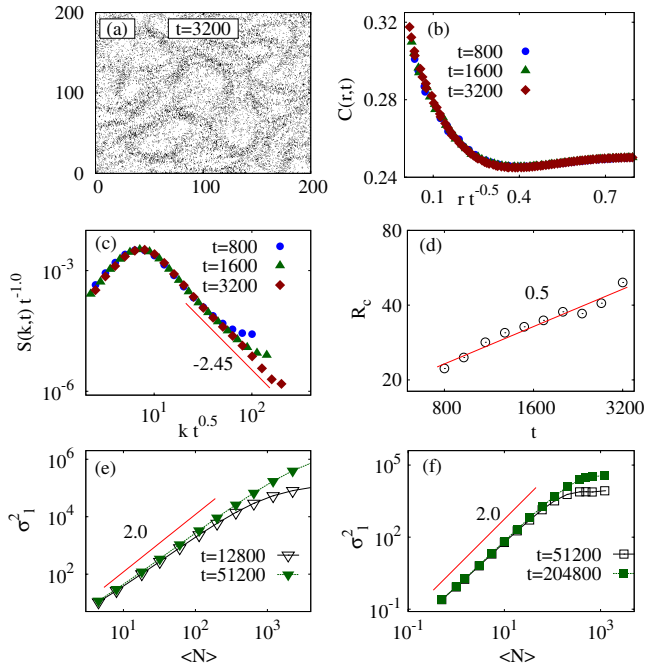

FIG. 2 (color online). (a)–(e) Simulation results for the AR model (system size 1024×1024, $\rho = 0.5$, $v_0 = 0.3$, and $\Lambda = 0.08$). (a) Snapshot of a part of the system at $t = 3200$ showing the domain structure. (b) $C(r, t)$ versus $r/\mathcal{L}(t)$ showing data collapse. (c) The scaled structure function is a power law with exponent -2.5 at large $k\mathcal{L}(t)$. (d) The mean cell radius $R_c(t) \sim \mathcal{L}(t)$. (e) Number fluctuations $\sigma_l^2 \sim \langle N\rangle^{2.0}$. (f) Sliding particle model (10^6 lattice sites, particle density 0.5): $\sigma_l^2 \sim \langle N\rangle^{2.0}$.

We make two important observations related to Eq. (3). First, the data in Figs. 2(e) and 2(f) and also in the experiment of vibrated granular rods [4], show a visible deviation from the leading $\sigma_l^2 = \langle N\rangle^2$ behavior. We claim that the subleading term in Eq. (3) may account for this deviation. We confirmed that $-\sigma_l^2/\langle N\rangle^2 + a$ indeed scale as $\langle N\rangle^{0.23}$ (consistent with $\beta_1 = 0.45$, $d = 2$) and $\langle N\rangle^{0.5}$ (consistent with $\beta_1 = 0.5$, $d = 1$), respectively, for the data in Figs. 2(e) and 2(f). More remarkably, we fitted the published experimental data [4] in this way (see the Supplementary Material [24]) and concluded that the experimental system has a $\beta_1 \approx 0.5$—that is, Porod's law is indeed violated and the exponent is close to the AR model above. We, thus, suggest that Eq. (3) opens up a new possibility for experimentalists—by measuring the subleading corrections to GNF, they can indirectly measure Porod's law violation. Second, we do not see a power law $\sim|\mathbf{k}|^{-2}$ at small $\mathbf{k}$ for $S(\mathbf{k})$ [see Fig. 2(c)], as suggested by continuum theory [17]. The same is true for the sliding particle model [20], as well as the clean phase separating system discussed above—for the latter $S(\mathbf{k}, t) = 4\mathcal{L}(t)\sin^2(k\mathcal{L}(t)/2)/(k\mathcal{L}(t))^2$.

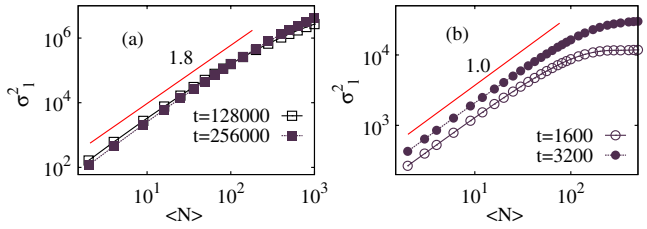

FIG. 3 (color online). Number fluctuations: (a) the granular gas ($L = 10^5$, $\rho = 1.0$, $r_0 = 0.5$, $\sigma = \infty$, and $\delta = 0.008$) showing GNF with exponent $\alpha = 1.8$. (b) ballistic aggregation ($L = 10^5$, and $\rho = 1.0$) shows normal fluctuation with exponent $\alpha = 1.0$.

Instead, these three examples have a divergence $\sim \mathcal{L}^d$ as $\mathbf{k} \to 0$. This indicates that $\sigma_l^2 \sim l^d S(\mathbf{k} \to 0) \sim l^{2d} \sim \langle N \rangle^2$.

Type 3.—A situation different from type 2 would arise if $C(\mathbf{r}, t)$ has a power law form $\sim |\mathbf{r}/\mathcal{L}(t)|^{-\eta}$ over small through large $|\mathbf{r}/\mathcal{L}(t)|$. On one hand, there will be non-Porod behavior, and on the other, the same exponent contributes to the GNF exponent α and is given by Eq. (2), provided $\eta < d$. Although we are not aware of an active matter system exhibiting such behavior, another nonequilibrium system, namely a freely cooling granular gas in one-dimension [21], serves as an example of this type. Its structure function shows that the $|\mathbf{k}|$ space exponent is -0.8 [21], and hence $\eta = 0.2$. We revisit this model, and calculate the $\sigma_l^2(t)$ in the coarsening regime. The result is shown in Fig. 3(a). We find a new GNF exponent value $\alpha = 1.8$, consistent with Eq. (2).

Type 4.—Central limit theorem, as in $\alpha = 1$, may hold in an interesting situation. This is when dense clusters (with masses scaling as $\mathcal{L}(t)^d$) appear in isolated locations, leading to temporal "intermittency." In this case, $C(\mathbf{r}, t) = \mathcal{L}(t)^d \delta(\mathbf{r}) + f(|\mathbf{r}/\mathcal{L}(t)|)$. Due to the presence of the δ-function, the form of the scaling function $f(|\mathbf{r}/\mathcal{L}(t)|)$ is irrelevant in the calculation of σ_l^2 from Eq. (1). Thus, $\alpha = 1$. Such situations arise in aggregation models, diffusive or ballistic, wherein particles aggregate on contact conserving mass. The density-density correlation function for the ballistic system has been studied in molecular dynamics and also for an equivalent lattice model [25]. For $|\mathbf{r}/\mathcal{L}(t)| > 0$, the scaling form of the correlation function starts from a low value, rises linearly and then saturates, with increasing $|\mathbf{r}/\mathcal{L}(t)|$. While Porod's law holds, $C(\mathbf{r}, t)$ also has a term $\mathcal{L}(t)\delta(\mathbf{r})$. We measure σ_l^2 in simulations of the lattice version of the model, and clearly see $\alpha = 1$ as predicted [see Fig. 3(b)]. We note that type 4 is distinct from the other types in another respect: $\langle N^k \rangle \propto \langle N \rangle$, for all integer $k \geq 2$, a consequence of statistics being dominated by the largest cluster. We check that this is true for ballistic aggregation. For all other cases (types 1–3) $\langle N^k \rangle \propto \langle N \rangle^{\gamma k}$, where the exponent γ is specific to a system.

In summary, we studied well known discrete models of active matter and some other nonequilibrium systems, to understand similarities and differences in their density structures. All the active matter systems that we studied were shown to violate Porod's law, and the non-Porod behavior is quantified by various new exponents. We categorized the relationship between spatial density-density correlation function and giant number fluctuation into four types. Unlike the classification of active matter systems based on microscopic symmetries (nematic, polar, etc.), our classification scheme is based on the *shapes* of the measured or calculated spatial density-density correlation functions during coarsening. The scheme is based on simple features in the shape, like presence or absence of a δ function at $r = 0$ (type 4), a power law divergence as $r/\mathcal{L}(t) \to 0$ (type 3), a finite approach as $r/\mathcal{L}(t) \to 0$ with a single-piece (type 2) or a two-piecewise (type 1) decay. Even if the scaled correlator has more than two-piece decay, then also as in type-1, the non-Porod exponent and number fluctuation exponent would be unrelated. In addition to active matter systems, we also bring some other nonequilibrium systems within the ambit of our classification. Among active matter systems, we show that polar particles and rods are of type 1, while apolar rods are of type 2. For polar systems, we identify a new coarsening length scale $\mathcal{L}(t) \sim t^{0.25}$. For apolar systems, we showed that the subleading corrections to the number fluctuations may help experimentalists to detect Porod's law violation. We demonstrate this by analyzing published data from the literature. We argue that the known discrete models belonging to type 2 exhibit GNF for a different reason than proposed by continuum theory of active nematics. We hope that this study will encourage experimentalists to probe density structures in detail in the future.

*supravat@phy.iitb.ac.in

[1] M. Ballerini *et al.*, Animal Behaviour **76**, 201 (2008); M. Ballerini *et al.*, Proc. Natl. Acad. Sci. U.S.A. **105**, 1232 (2008).
[2] H. P. Zhang, A. Beér, E.-L. Florin, and H. L. Swinney, Proc. Natl. Acad. Sci. U.S.A. **107**, 13 626 (2010).
[3] V. Schaller, C. Weber, C. Semmrich, E. Frey, and A. R. Bausch, Nature (London) **467**, 73 (2010).
[4] V. Narayan, S. Ramaswamy, and N. Menon, Science **317**, 105 (2007).
[5] A. Kudrolli, G. Lumay, D. Volfson, and L. S. Tsimring, Phys. Rev. Lett. **100**, 058001 (2008).
[6] J. Deseigne, O. Dauchot, and H. Chaté, Phys. Rev. Lett. **105**, 098001 (2010).
[7] T. Vicsek, A. Czirók, E. Ben-Jacob, I. Cohen, and O. Shochet, Phys. Rev. Lett. **75**, 1226 (1995); T. Vicsek and A. Zafiris, arXiv:1010.5017.
[8] Y. Tu, J. Toner, and M. Ulm, Phys. Rev. Lett. **80**, 4819 (1998).
[9] G. Grégoire and H. Chaté, Phys. Rev. Lett. **92**, 025702 (2004); H. Chaté, F. Ginelli, G. Grégoire, and F. Raynaud, Phys. Rev. E **77**, 046113 (2008).
[10] H. Chaté, F. Ginelli, and R. Montagne, Phys. Rev. Lett. **96**, 180602 (2006).

[11] F. Ginelli, F. Peruani, M. Bär, and H. Chaté, Phys. Rev. Lett. **104**, 184502 (2010).
[12] F. Ginelli and H. Chaté, Phys. Rev. Lett. **105**, 168103 (2010).
[13] J. Toner and Y. Tu, Phys. Rev. Lett. **75**, 4326 (1995).
[14] J. Toner, Y. Tu, and S. Ramaswamy, Ann. Phys. (N.Y.) **318**, 170 (2005).
[15] A. Baskaran and M. C. Marchetti, Phys. Rev. Lett. **101**, 268101 (2008); A. Baskaran and M. C. Marchetti, Phys. Rev. E **77**, 011920 (2008).
[16] F. Peruani, A. Deutsch, and M. Bär, Phys. Rev. E **74**, 030904 (2006).
[17] S. Ramaswamy, R. Aditi Simha, and J. Toner, Europhys. Lett. **62**, 196 (2003).
[18] A. J. Bray, Adv. Phys. **43**, 357 (1994).
[19] G. Porod, *Small-Angle X-ray Scattering* (Academic, London, 1982).
[20] D. Das and M. Barma, Phys. Rev. Lett. **85**, 1602 (2000); D. Das, M. Barma, and S. N. Majumdar, Phys. Rev. E **64**, 046126 (2001); G. Manoj and M. Barma, J. Stat. Phys. **110**, 1305 (2003).
[21] M. Shinde, D. Das, and R. Rajesh, Phys. Rev. Lett. **99**, 234505 (2007); M. Shinde, D. Das, and R. Rajesh, Phys. Rev. E **84**, 031310 (2011).
[22] S. Mishra and S. Ramaswamy, Phys. Rev. Lett. **97**, 090602 (2006); S. Mishra, F. Ginelli, H. Chaté, S. Puri, and S. Ramaswamy (unpublished).
[23] S. Mishra, A. Baskaran, and M. C. Marchetti, Phys. Rev. E **81**, 061916 (2010).
[24] See Supplemental Material at http://link.aps.org/supplemental/10.1103/PhysRevLett.108.238001. for details.
[25] S. Dey, D. Das, and R. Rajesh, Europhys. Lett. **93**, 44001 (2011); M. Shinde, D. Das, and R. Rajesh, Phys. Rev. E **79**, 021303 (2009).